Tetrahedron 68 (2012) 6054–6058

Contents lists available at SciVerse ScienceDirect

Tetrahedron

journal homepage: www.elsevier.com/locate/tet

Morusalbanol A, a neuro-protective Diels–Alder adduct with an unprecedented architecture from *Morus alba*

Hua-Dong Chen [a], Yuan-Qing Ding [b], Sheng-Ping Yang [a], Xing-Cong Li [b], Xu-Jie Wang [a], Hai-Yan Zhang [a], Daneel Ferreira [b], Jian-Min Yue [a,*]

[a] *State Key Laboratory of Drug Research, Institute of Materia Medica, Shanghai Institutes for Biological Sciences, Chinese Academy of Sciences, 555 Zuchongzhi Road, Zhangjiang Hi-Tech Park, Shanghai 201203, PR China*

[b] *National Center for Natural Products Research, Research Institute of Pharmaceutical Sciences, and Department of Pharmacognosy, School of Pharmacy, The University of Mississippi, University, MS 38677, USA*

ARTICLE INFO

Article history:
Received 2 March 2012
Received in revised form 24 April 2012
Accepted 4 May 2012
Available online 12 May 2012

Keywords:
Morus alba
Natural products
Morusalbanol A
Absolute configuration
Neuro-protective activity

ABSTRACT

Morusalbanol A (**1**), a neuro-protective Diels–Alder adduct with a new carbon skeleton, was isolated from the bark of *Morus alba*. Compound **1** showed evidence of interesting astropisomerism, and resulted in the absence of a number of key proton and carbon signals in the NMR spectra. Its structure was thus elucidated by spectroscopic analysis of its peracetylated derivative (**2**) and its absolute configuration established as 1*S*,3*S*,4*R*,5*S* via experimental and calculated ECD spectra of **1**. In a neuro-protective assay, morusalbanol A (**1**) significantly attenuated the H_2O_2-induced cell damage in a dose-dependent manner.

1. Introduction

The plant *Morus alba* L. (Moraceae) is widely distributed in China.[1] and its bark has been used in Traditional Chinese Medicine (TCM) to purge lung-fire, relieve dyspnea, promote dieresis, and lower blood pressure.[2] Previous chemical investigations on *M. alba* led to the identification of an array of isoprenoid-substituted phenolics,[3] organic acids,[4] sugars,[5] and alkaloids.[6] In particular, the isoprene-substituted flavanone derivatives exhibit a variety of significant biological activities. These derivatives are presumably Diels–Alder adducts of a chalcone and isoprenylflavanone moieties.[7] In the current study, a Diels–Alder adduct, morusalbanol A (**1**) (Fig. 1), with an unprecedented carbon skeleton, was isolated from the bark of *M. alba*. Morusalbanol A (**1**) showed evidence of astropisomerism, and resulted in the absence of a number of key proton and carbon signals in the NMR spectra. Its peracetylated derivative **2** was thus used for the structural assignment of **1**. In the neuro-protective activity bioassay, morusalbanol A (**1**) at 2.5, 5, and 10 μM significantly attenuated the H_2O_2-induced cell damage in a dose-dependent manner. We report herein the isolation, structural elucidation, and neuro-protective activity of compound **1**.

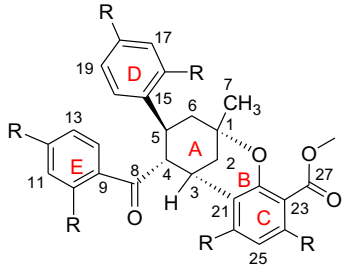

1 R = OH
2 R = OAc

2. Results and discussion

2.1. Structural elucidation

Morusalbanol A (**1**), a yellow powder, gave the molecular formula $C_{28}H_{26}O_{10}$ as determined by HRESIMS at *m*/*z* 545.1423 $[M+Na]^+$ (calcd for $C_{28}H_{26}O_{10}Na$, 545.1424) and ^{13}C NMR data. The UV maxima at 201, 221, 276, and 312 nm, and IR absorptions at 3384, 1608, 1452, and 1146 cm^{-1} suggested the presence of similar

* Corresponding author. Tel./fax: +86 21 50806718; e-mail address: jmyue@mail.shcnc.ac.cn (J.-M. Yue).

0040-4020/$ – see front matter © 2012 Elsevier Ltd. All rights reserved.
doi:10.1016/j.tet.2012.05.017

chromophores and functional groups as those of cathayanon A.[7d] However, several proton and carbon resonances were absent in the ^{1}H and ^{13}C NMR spectra recorded at room temperature in methanol-d_4 (two proton and seven carbon resonances not visible) and DMSO-d_6 (two proton and four carbon resonances not visible). When the spectra were recorded in DMSO-d_6 at 353 K, one proton and one carbon resonance were still invisible (Table 1). These NMR phenomena were most likely caused by astropisomerism of **1** in solution. Thus, compound **1** was acetylated with acetic anhydride in pyridine to give compound **2** that gave well-resolved ^{1}H and ^{13}C NMR spectra. Comparison of the ^{13}C NMR data (Fig. 1) of rings A–E of compounds **1** and **2** showed high consistency, indicating that the carbon skeleton and stereochemistry of **1** were kept unchanged in the acetylation. Further analysis of the spectroscopic data (Table 1) of compound **2** revealed that it is the peracetylated derivative of **1**.

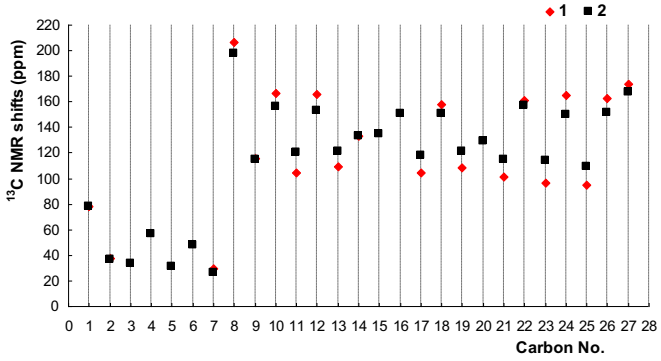

Fig. 1. Comparison of the ^{13}C NMR data of stereogenic centers of **1** and **2**.

Compound **2** was obtained as colorless powder, $[\alpha]_D^{23}+30$ (*c* 0.03, MeOH), and its HRESIMS data at *m*/*z* 797.2000 $[M+Na]^+$ and ^{13}C NMR data corresponded to the molecular formula $C_{40}H_{38}O_{16}$ (calcd for $C_{40}H_{38}O_{16}Na$, 797.2058) requiring 22 degrees of unsaturation. Its ^{1}H and ^{13}C NMR spectra (Table 1) indicated, besides the proton and carbon resonances attributable to six *O*-acetyl and an *O*-methoxyl groups, the presence of a keto carbonyl and an ester carbonyl groups, three aromatic rings (two ABX systems and a pentasubstituted ring), a methyl, two sp^3 methylene, three sp^3 methine, and an oxygenated sp^3 quaternary carbon (δ_C 78.2 s). Two ABX systems corresponding to the D- and E-rings were readily recognized by ^{1}H NMR, $^{1}H-^{1}H$ COSY, and HMBC spectra (Fig. 2). A proton coupling network from H-2 to H-6 revealed by the $^{1}H-^{1}H$ COSY spectrum was further supported by the HMBC correlations from H_3-7 to C-1, C-2, and C-6 (Fig. 2), indicating the presence of a tetrasubstituted methylcyclohexane ring, which was different from the trisubstituted methylcyclohexene core of cathayanon A.[7d] The presence of a 2,3,4,6-tetrasubstituted methyl benzoate moiety (ring C) was revealed by the NMR data (Table 1) and the HMBC correlations. The methoxycarbonyl group was attached at C-23 by the chemical shift at δ_C 114.0 and a weak HMBC correlation between H-25 and C-27 (a W-type long-range proton–carbon coupling), which was supported by the well matched NMR data of the ring C of **1** versus those of the similar 2,3,4,5,6-pentasubstituted patterns of benzene moieties found in sanggenols L and M,[7a] and cathayanons A and B.[7d] Furthermore, the HMBC correlations of H-14/C-8, H-4/C-8, and H-4/C-9 connected A- and E-rings via the C-8 keto group; the HMBC correlations from H-5 to C-15 and C-16 attached D-ring to C-5; and the HMBC correlations from both H-3 and H-4 to C-21 linked A- and C-rings via the C-3–C-21 bond. The A-, C-, D- and E-rings and the six *O*-acetyl groups accounted for 21 out of the 22 degrees of unsaturation in **2**; the remaining one required the presence of an additional ring. The quaternary carbon resonance at δ_C 78.2 (C-1) and the downfield shifted olefinic carbon resonance at δ_C 157.0 (C-22) suggested their linkage via an ether bond to form the B-ring. This was confirmed by a weak but key HMBC correlation between H_3-7 and C-22 (also a W-type long-range $^{4}J_{CH}$ coupling). The six *O*-acetyl groups could only be placed at C-10, C-12, C-16, C-18, C-24, and C-26, respectively. The planar structure of **2** was thus fully defined and represented an unprecedented carbon skeleton.

The relative configuration of **2** was determined by analysis of the coupling constants (Table 1) and the NOESY spectrum (Fig. 2). The large coupling constant (11.8 Hz) between H-4 and H-5 clearly indicated their *trans*-diaxial arrangement. The small coupling constant (3.0 Hz) between H-3 and H-4 showed their *cis*-orientation with H-3 in an equatorial position. In the NOESY spectrum (Fig. 2), the correlations of H-2β/H-4, H-4/H-3, H-4/H-6β, and H_3-7/H-2β, and H-6β indicated that they were cofacial, and randomly assigned in a β-orientation. This analysis also revealed that rings A and B adopted chair-like and half-chair conformations, respectively. The relative configuration of **2** is consistent with those of the Diels–Alder *cis–trans* adducts via *endo*-addition from Moraceous plants.[8]

Theoretical calculation of the electronic circular dichroism (ECD) spectrum[9] was applied to determine the absolute configuration of compound **1**. The arbitrarily assigned 1*S*,3*S*,4*R*,5*S* absolute configuration was chosen for a systematic conformational random search by using the MMFF94 method in Sybyl 8.1. Thirty-one conformers were found by molecular mechanics force-field calculation with an energy cut-off of 15 kcal/mol. The first seven conformers within the energy cut-off of 5 kcal/mol were included for the full geometry optimization at the B3LYP/6-31G** level in the gas phase. Four conformers, **1a**–**1d** (Fig. 3), were relocated with a Boltzman distribution of 91.8, 3.2, 0, and 4.9%, calculated by relative energy with zero point energy (ZPE) in the gas phase (Table 2). All four conformers adopt a chair and half-chair conformations for the A- and B-rings, respectively (Fig. 3), the only differences being the orientation of the D-ring and the C-23 methoxycarbonyl group. Such conformations plausibly explain the experimentally observed NOE correlations. Next, the ECD spectra of individual conformers were calculated by using time-dependent density functional theory (TDDFT) at the B3LYP/6-311++G**//B3LYP/6-31G** level in the gas phase. Using the predominant conformer **1a**, the experimentally observed strong positive Cotton effect (CE) in the 280–350 nm region is attributed to the electronic transitions at 304 and 352 nm (Fig. 4), the positive CE (shoulder) at 275 nm by the transitions at 264, 260, and 254 nm, and the negative CE at 234 nm by the transitions at 233 and 228 nm. The overall consistency of the calculated and experimental ECD spectra supports the absolute configuration of **1** as 1*S*,3*S*,4*R*,5*S*.

Computationally calculated conformations of compound **1** (Fig. 3) permitted a better understanding of the astropisomerism observed in the measurement of its NMR spectra. The absence of a number of proton (H-3 and H-5) and carbon (C-3, C-4, C-5, C-6, C-15, C-16, and C-20) resonances in methanol-d_4 at ambient temperature presumably resulted from interconversions of several astropisomers due to the rotational hindrance of the D/E-rings about the C-5–C-15 and C-4–C-8–C-9 bonds. The intramolecular hydrogen bonding between the C-8 carbonyl group and the C-16 and C-26 hydroxy groups may also significantly contributed to the rotational restrictions. This hindered rotation was slightly relieved in DMSO-d_6 (resonances of H-3 and H-5 and C-3, C-5, C-15, and C-20 were absent). At an elevated temperature (353 K), the H-5 and C-5 were still invisible (Table 1). Principally, there are two methods to ameliorate the adverse NMR effects of hindered rotation, i.e., to induce free rotation by temperature elevation, or to completely inhibit rotation by temperature decrease or to increase the bulk of substituents close to the axis in order to prevent conformational exchange. When the NMR spectra of **1** were acquired at 353 K in

Table 1
^{1}H and ^{13}C NMR data of compounds **1** and **2**

No.	**1**[a]		**1**[b]		**1**[c]		**2**[a]	
	δ_C	δ_H (pattern, J/Hz)	δ_C	δ_H (pattern, J/Hz)	δ_C	δ_H (pattern, J/Hz)	δ_C	δ_H (pattern, J/Hz)
1	77.8		75.6		75.5		78.2	
2	37.2	2.24 (dd, 12.0, 2.7) 1.74 (d, 12.0)	35.2	2.27 (brd, 12.0) 1.61 (brd, 12.0)	35.2	2.26 (dd, 12.8, 2.3) 1.75 (d, 12.8)	36.3	1.92 (ddd, 13.5, 2.8, 2.6) 2.39 (dd, 13.5, 2.8)
3	[d]	[d]	[d]	[d]	49.8	4.37 (d, 2.3)	33.1	3.68 (dt, 3.0, 2.8)
4	[d]	3.63 (2.7)	30.4	3.51 (brd)	30.3	3.51 (d, 2.4)	56.8	4.24 (dd, 11.8, 3.0)
5	[d]	[d]	[d]	[d]	[d]	[d]	30.7	3.48 (ddd, 13.0,11.8, 4.2)
6	[d]	2.11 (br s)	49.6	1.98 (br s)	45.5	2.05 (brd, 13.0) 1.75 (brd, 13.0)	47.8	2.07 (ddd, 13.5, 4.2, 2.6) 1.77 (dd, 13.5, 13.0)
7	29.5	1.40 (s)	28.3	1.29 (s)	28.1	1.34 (s)	26.6	1.41 (s)
8	206.7		204.2		204.0		197.7	
9	115.8		113.4		113.5		114.8	
10	166.9		164.1		164.0		156.3	
11	104.1	6.18 (2.6)	102.3	6.14 (d, 2.7)	102.3	6.18 (d, 2.4)	120.2	6.98 (d, 2.4)
12	165.9		163.8		163.6		152.9	
13	109.0	6.39 (dd, 8.9, 2.6)	107.5	6.39 (dd, 8.7, 2.7)	107.4	6.41 (dd, 8.9, 2.4)	121.3	7.19 (dd, 8.7, 2.4)
14	133.4	7.94 (d, 8.9)	131.9	8.06 (br s)	131.7	8.01 (d, 8.9)	133.1	8.16 (d, 8.7)
15	[d]		[d]		120.5		134.4	
16	[d]		155.3		155.2		150.6	
17	104.6	6.17 (d, 2.3)	102.3	6.12 (d, 2.6)	102.7	6.17 (d, 2.4)	118.0	6.79 (d, 2.4)
18	157.7		155.7		155.7		151.0	
19	108.2	6.11 (dd, 8.4, 2.3)	105.8	5.95 (dd, 8.3, 2.6)	105.9	6.02 (dd, 8.3, 2.4)	121.0	6.81 (dd, 8.3, 2.4)
20	[d]	6.80 (d, 8.4)	[d]	6.73 (br s)	127.9	6.74 (d, 8.3)	129.1	7.24 (d, 8.3)
21	101.5		101.4		101.5		114.8	
22	160.7		157.2		157.4		157.0	
23	96.1		96.2		95.9		114.0	
24	164.8		159.4		159.8		149.8	
25	95.1	5.78 (s)	93.3	5.77 (s)	93.4	5.81 (s)	109.4	6.50 (s)
26	162.7		159.4		159.4		151.8	
27	173.9		169.8		169.8		167.2	
CH_3O	52.5	3.85 (s)	51.7	3.74 (s)	51.2	3.79 (s)	53.2	3.86 (s)
AcO							171.5	2.28 (s)
							171.4	2.21 (s)
							171.3	2.20 (s)
							170.6	2.20 (s)
							170.6	2.18 (s)
							170.4	1.51 (s)
							21.4	
							21.3	
							21.3	
							21.1	
							20.8	
							14.9	

[a] In methanol-d_4.
[b] In DMSO-d_6 at 298 K.
[c] In DMSO-d_6 at 353 K.
[d] Signals invisible.

DMSO-d_6, the H-5 and C-5 resonances were still missing, indicating that this temperature was not sufficient to overcome the rotational restrictions. The second strategy was thus pursued by acetylation of **1** to yield the per-*O*-acetyl derivative **2**, which gave well-resolved ^{1}H and ^{13}C NMR spectra (Table 1) at ambient temperature.

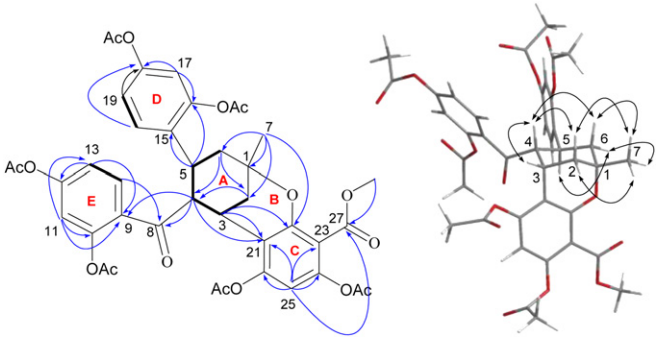

Fig. 2. Selected $^{1}H-^{1}H$ COSY (▬), HMBC (H→C) and NOESY correlations (↔) of **2**.

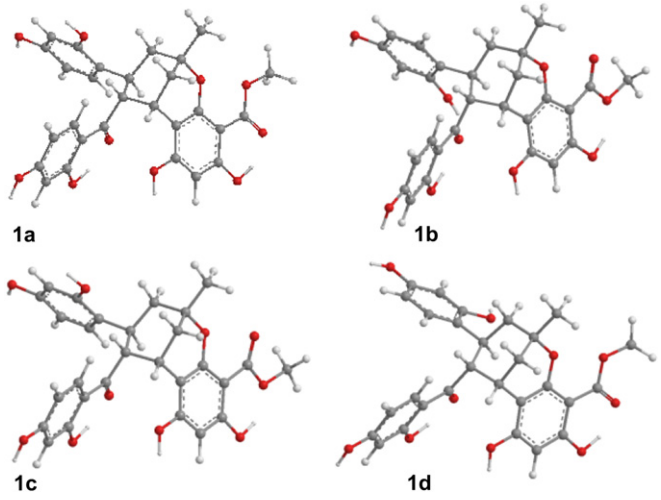

Fig. 3. Optimized geometries of predominant conformers of **1** at the B3LYP/6-31G* level in the gas phase.

Table 2
Conformational analysis of compound **1** in the gas phase

Species	ΔE^{a}	$P_E\%^{b}$	$\Delta E'^{a}$	$P_{E'}\%^{b}$	ΔG^{a}	$P_G\%^{b}$	$\Delta E''^{c}$	$P_{E''}\%^{c}$
1a	0.00	90.0	0.00	91.8	0.00	90.3	0.00	85.1
1b	1.66	5.5	1.98	3.2	2.09	2.7	1.31	9.3
1c	5.05	0.0	4.94	0.0	4.29	0.1	3.88	0.1
1d	1.77	4.5	1.73	4.9	1.51	7.0	1.63	5.5

[a] Relative energy, relative energy with ZPE, and relative Gibbs free energy at the B3LYP/6-31G** level in the gas phase, respectively (kcal/mol).
[b] Conformational distribution calculated by using the respective parameters above at the B3LYP/6-31G** level in the gas phase.
[c] Relative energy (kcal/mol) and conformational distribution at the B3LYP/6-311++G**//B3LYP/6-31G** level in the gas phase, respectively.

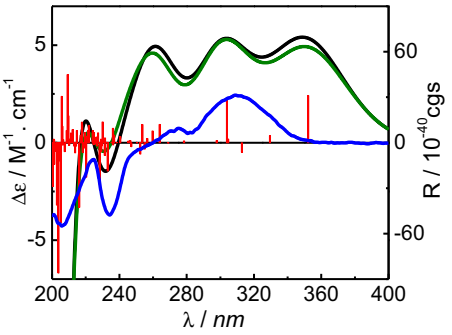

Fig. 4. Experimental (blue, in MeOH) and calculated ECD spectra of compound **1** at the B3LYP/6-311++G**//B3LYP/6-31G** level in the gas phase: black, weighted; red, calculated rotatory strengths of predominant conformer **1a**; and olive, simulated ECD curve of predominant conformer **1a**.

A possible biosynthetic pathway toward the formation of **1** was postulated in Scheme 1. Oxidative degradation and methylation of a prenylated chalcone-type compound **i** would give key precursor **ii**. Diels–Alder *endo*-addition of **ii** with another chalcone-type compound **iii** would produce intermediate **iv** as *cis–trans* adduct. This is similar to the mechanism proposed for the formation of a number of Diels–Alder-type adducts isolated from *Morus* plants via coupling of a chalcone moiety with a prenylated flavonoid derivative.[8] The intermediate **iv** would be susceptible to acid-catalyzed regio- and stereo-selective intramolecular cyclization to form compound **1**.[10]

The cell protecting activity against H_2O_2-induced PC12 cell damage of **1**, was evaluated according to the reported protocol[11] with minor modification. After exposure to 300 μM H_2O_2, cell viability as determined by MTT reduction was markedly decreased to 67% ($^{\#\#}P<0.01$ vs control). However, pretreatment with compound **1** at 1, 2.5, 5, and 10 μM significantly attenuated the H_2O_2-induced cell damage ($^{**}P<0.01$ vs H_2O_2 group) in a dose-dependent manner (Fig. 5).

3. Conclusions

The discovery of a major component morusalbanol A (**1**) from the bark of *Morus alba*, a common traditional Chinese medicine (TCM), is much important for the TCM standardization and quality control. Morusalbanol A, a Diels–Alder adduct of new carbon skeleton showed the evidence of astropisomerism and significant neuro-protective activity, which might be the interesting topics for both synthetic chemistry and pharmacology in the future.

4. Experimental section

4.1. General experimental procedures

Optical rotations were determined on a Perkin–Elmer 341 polarimeter, and CD spectra were obtained on a Jasco 810 spectrometer.

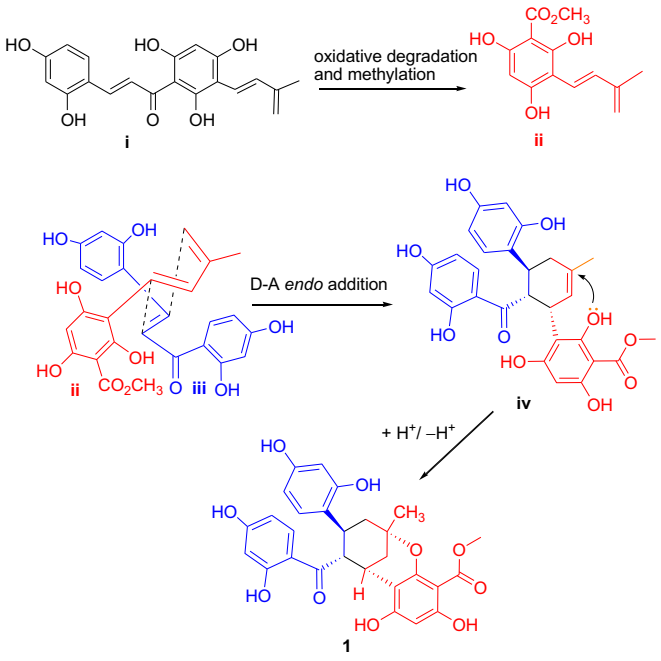

Scheme 1. Plausible biogenetic pathway proposed for morusalbanol A (**1**).

IR spectra were recorded on a Perkin–Elmer 577 spectrometer with KBr disks. NMR spectra were acquired on a Bruker AM-400 spectrometer. EIMS (70 eV) were carried out on a Finnigan MAT 95 mass spectrometer. ESIMS and HRESIMS were obtained on an Esquire 3000plus (Bruker Daltonics) and a Waters-Micromass Q-TOF Ultima Global electrospray mass spectrometer, respectively. Silica gel

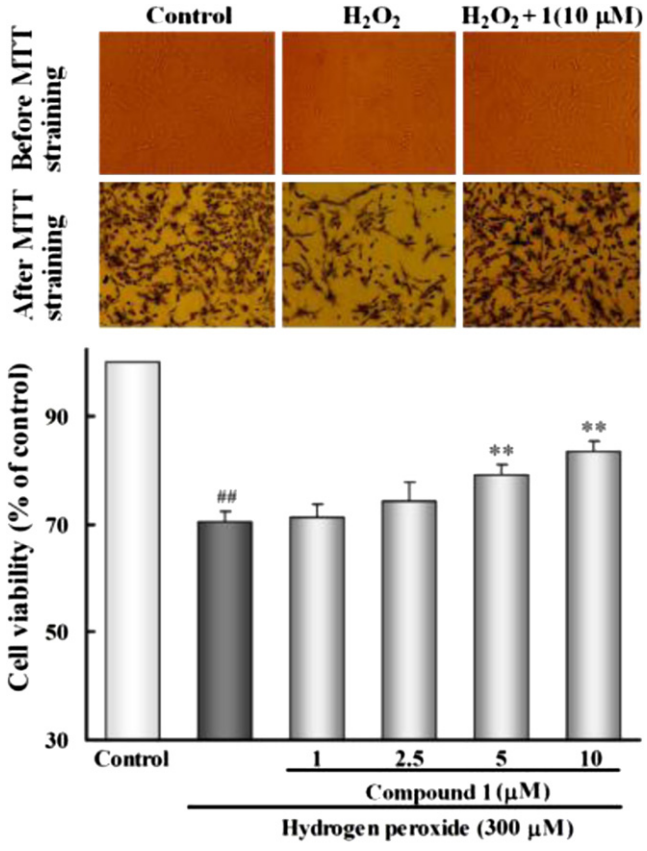

Fig. 5. Effects of morusalbanol A (**1**) on cell viability.

(200–300 mesh) (Qingdao Haiyang Chemical Co. Ltd.), C18 reverse-phased silica gel (150–200 mesh, Merck), MCI gel (CHP20P, 75–150 μM, Mitsubishi Chemical Industries Ltd.) were used for column chromatography. All solvents used were of analytical grade (Shanghai Chemical Plant, Shanghai, PR China).

4.2. Plant material

The *M. alba* L. plant material was collected from Hunan Province of the People's Republic of China, and was authenticated by Professor Zheng-Tao Wang of Shanghai University of Traditional Chinese Medicine. A voucher specimen (accession number MAL-2004-3Y) has been deposited in the Shanghai Institute of *Materia Medica*.

4.3. Extraction and isolation

The powder of the root bark of *M. alba* (2.5 kg) was extracted with 95% EtOH at ambient temperature to give a dark crude extract (300 g), which was partitioned between EtOAc and H_2O. The EtOAc-soluble portion (113 g) was subjected to column chromatography on silica gel using petroleum ether–acetone mixtures of increasing polarity. The fraction that eluted with petroleum ether–acetone (3:1) was subjected to CC on MCI gel (MeOH/H_2O, 4:6–9:1) to obtain a major fraction (5.1 g), which was first separated over a column of silica gel eluted with $CHCl_3$/MeOH (20:1), and then the major component (0.6 g) was purified by CC on RP-18 silica gel (50% MeOH in H_2O) to afford **1** (81 mg).

*4.3.1. Morusalbanol A (**1**).* Yellow powder; $[\alpha]_D^{23}$+163 (*c* 0.12, MeOH); UV (MeOH) λ_{max} (log ε) 201 (4.59), 221 (4.55), 276 (4.42), 312 (3.99) nm; CD (MeOH) $\Delta\varepsilon_{206}$ −4.27, $\Delta\varepsilon_{225}$−0.86, $\Delta\varepsilon_{234}$−3.70, $\Delta\varepsilon_{275}$+0.74, $\Delta\varepsilon_{281}$+0.47, $\Delta\varepsilon_{309}$+2.43; IR (KBr) ν_{max} 3385, 2972, 1608, 1510, 1443, 1321, 1242, 1157, 1095, 975, 806, 624 cm^{-1}; for ^1H and ^{13}C NMR data, see Table 1; positive ESIMS *m/z* 545.2 $[M+Na]^+$, 1067.3 $[2M+Na]^+$, negative ESIMS *m/z* 521.2 $[M-H]^-$, 1043.4 $[2M-H]^-$; HRESIMS *m/z* 545.1423 $[M+Na]^+$ (calcd for $C_{28}H_{26}O_{10}Na$ 545.1424).

*4.3.2. Preparation of compound **2**.* To a solution of pyridine (3 mL) containing 8.0 mg of compound **1**, 0.5 mL of acetic anhydride was added. The mixture was stirred for 8 h at room temperature. After removal of the solvents under reduced pressure, the residue was purified by a silica gel column eluted with petroleum/EtOAc (4:1) to give compound **2** (8.5 mg). Compound **2**: white powder; $[\alpha]_D^{23}$+30 (*c* 0.03, MeOH); UV (MeOH) λ_{max} (log ε) 198 (4.74), 240 (4.03), 250 (4.06), 304 (3.83) nm; CD (MeOH) $\Delta\varepsilon_{204}$−0.42, $\Delta\varepsilon_{216}$−1.47, $\Delta\varepsilon_{285}$+0.48; IR (KBr) ν_{max} 3423, 2920, 1772, 1606, 1201, 1093 cm^{-1}; for ^1H and ^{13}C NMR data, see Table 1; positive ESIMS *m/z* 797.3 $[M+Na]^+$; HRESIMS *m/z* 797.2000 $[M+Na]^+$ (calcd for $C_{40}H_{38}O_{16}Na$ 797.2058).

4.4. Methods of computational calculations

The theoretical calculations were performed by the SYBYL 8.1 program (Tripos International, St. Louis, MO) and the Gaussian03 program package.[12] MMFF94 molecular mechanics force-field was employed to search the possible conformations. All ground-state geometries were optimized at the B3LYP/6-31G** level at 298 K, and harmonic frequency analysis was computed to confirm the minima. TDDFT at the B3LYP/6-311++G**//B3LYP/6-31G** level in the gas phase was employed to calculate excitation energy (in nm) and rotatory strength *R* (velocity form R^{vel} and length form R^{len} in 10^{-40} erg-esu-cm/Gauss) between different states. The ECD spectra were simulated by overlapping Gaussian functions for each transition according to $\Delta\in(E) = (1/2.297\times10^{-39})(1/\sqrt{2\pi\sigma})\sum_i^A \Delta E_i R_i e^{-[(E-\Delta E_i)/(2\sigma)]^2}$ where σ is the width of the band at $1/e$ height and ΔE_i and R_i are the excitation energies and rotatory strengths for transition *i*, respectively. In this work, σ=0.15 eV was used.

4.5. Bioassay

Cells were incubated with 300 μM H_2O_2, and the cultures were developed for another 24 h in fresh medium. Compounds were added to the cultures 2 h prior to H_2O_2 addition. Three independent experiments were carried out in triplicate. All data were expressed as percentage of the control value. Statistical comparison was made by using one way ANOVA followed by Duncan's test. The data are expressed as means+SEM; $^{\#\#}P<0.01$ versus control; $^{**}P<0.01$ versus H_2O_2 group.

Acknowledgements

Financial support of the National Natural Science Foundation (Grant No. 81021062; 20932007) of the People's Republic of China is gratefully acknowledged. This work was also supported in part by the USDA Agricultural Research Service Specific Cooperative Agreement No. 58-6408-2-0009. We thank Professor Z.-T. Wang, Shanghai University of Traditional Chinese Medicine, for the identification of the plant material. We thank the Mississippi Center for Supercomputing Research (MCSR) for computational facilities.

Supplementary data

Supplementary data associated with this article can be found, in the online version, at doi:10.1016/j.tet.2012.05.017.

References and notes

1. Zhang, X. S.; Wu, Z. Y. *Flora of China (Zhongguo Zhiwu Zhi)*; Science: Beijing, 1998; vol. 23, pp 6–9.
2. State Administration of Traditional Chinese Medicine. *Chinese Herb (Zhonghua Bencao)*; Shanghai Science and Technology: Shanghai, 1999; vol. 2; 525–528.
3. (a) Nomura, T. *Pure Appl. Chem.* **1999**, *71*, 1115; (b) Nomura, T. *Yakugak Zasshi* **2001**, *121*, 535; (c) Du, J.; He, Z. D.; Jiang, R. W.; Ye, W. C.; Xu, H. X.; Paul, P. H. *Phytochemistry* **2003**, *62*, 1235; (d) Deshpande, V. H.; Parthasarathy, P. C.; Venkataramn, K. *Tetrahedron Lett.* **1968**, *9*, 1715.
4. Hatanaka, S. I.; Kaneko, S. *Phytochemistry* **1977**, *16*, 1041.
5. Asano, N.; Oseki, K.; Tomioka, E.; Kizu, H.; Matsui, K. *Carbohydrate Res.* **1994**, *259*, 243.
6. Asano, N.; Yamashita, T.; Yasuda, K.; Ikeda, K.; Kizu, H.; Kameda, Y.; Kato, A.; Nash, R. J.; Lee, H. S.; Ryu, K. S. *J. Agric. Food Chem.* **2001**, *49*, 4208.
7. (a) Shi, Y. Q.; Fukai, T.; Sakagami, H.; Chang, W. J.; Yang, P. Q.; Wang, F. P.; Nomura, T. *J. Nat. Prod.* **2001**, *64*, 181; (b) Nomura, T.; Fukai, T.; Hano, Y.; Uzawa, J. *Heterocycles* **1982**, *17*, 381; (c) Nomura, T.; Fukai, T.; Hano, Y.; Uzawa, J. *Heterocycles* **1981**, *16*, 2141; (d) Shen, R. C.; Lin, M. *Phytochemistry* **2001**, *57*, 1231.
8. Nomura, T.; Hano, Y. *Nat. Prod. Rep.* **1994**, *11*, 205.
9. (a) Diedrich, C.; Grimme, S. *J. Phys. Chem. A* **2003**, *107*, 2524; (b) Ding, Y.; Li, X.-C.; Ferreira, D. *J. Org. Chem.* **2007**, *72*, 9010; (c) Ding, Y.; Li, X.-C.; Ferreira, D. *J. Nat. Prod.* **2009**, *72*, 327; (d) Ding, Y.; Li, X.-C.; Ferreira, D. *J. Nat. Prod.* **2010**, *73*, 435.
10. Dewick, P. M. *Medicinal Natural Products: A Biosynthetic Approach*, 2nd ed.; John Wiley: Chichester, 2004, pp 175.
11. Wang, R.; Xiao, X. Q.; Tang, X. C. *Neuroreport* **2001**, *12*, 2629.
12. Frisch, M. J.; Trucks, G. W.; Schlegel, H. B.; Scuseria, G. E.; Robb, M. A.; Cheeseman, J. R.; Montgomery, J. A., Jr.; Vreven, T.; Kudin, K. N.; Burant, J. C.; Millam, J. M.; Iyengar, S. S.; Tomasi, J.; Barone, V.; Mennucci, B.; Cossi, M.; Scalmani, G.; Rega, N.; Petersson, G. A.; Nakatsuji, H.; Hada, M.; Ehara, M.; Toyota, K.; Fukuda, R.; Hasegawa, J.; Ishida, M.; Nakajima, T.; Honda, Y.; Kitao, O.; Nakai, H.; Klene, M.; Li, X.; Knox, J. E.; Hratchian, H. P.; Cross, J. B.; Adamo, C.; Jaramillo, J.; Gomperts, R.; Stratmann, R. E.; Yazyev, O.; Austin, A. J.; Cammi, R.; Pomelli, C.; Ochterski, J. W.; Ayala, P. Y.; Morokuma, K.; Voth, G. A.; Salvador, P.; Dannenberg, J. J.; Zakrzewski, V. G.; Dapprich, S.; Daniels, A. D.; Strain, M. C.; Farkas, O.; Malick, D. K.; Rabuck, A. D.; Raghavachari, K.; Foresman, J. B.; Ortiz, J. V.; Cui, Q.; Baboul, A. G.; Clifford, S.; Cioslowski, J.; Stefanov, B. B.; Liu, G.; Liashenko, A.; Piskorz, P.; Komaromi, I.; Martin, R. L.; Fox, D. J.; Keith, T.; Al-Laham, M. A.; Peng, C. Y.; Nanayakkara, A.; Challacombe, M.; Gill, P. M. W.; Johnson, B.; Chen, W.; Wong, M. W.; Gonzalez, C.; Pople, J. A. *Gaussian 03, Revision B. 02*; Gaussian: Pittsburgh PA, 2003.